JOURNAL OF PROPULSION AND POWER
Vol. 17, No. 1, January–February 2001

Technical Notes

TECHNICAL NOTES are short manuscripts describing new developments or important results of a preliminary nature. These Notes cannot exceed 6 manuscript pages and 3 figures; a page of text may be substituted for a figure and vice versa. After informal review by the editors, they may be published within a few months of the date of receipt. Style requirements are the same as for regular contributions (see inside back cover).

Fluid Property Effects on Sheet Disintegration of a Simplex Pressure-Swirl Atomizer

I-Ping Chung* and Cary Presser†
National Institute of Standards and Technology, Gaithersburg, Maryland 20899-8360

Introduction

WHEN describing liquid atomization, the process contains two basic stages, primary atomization and secondary atomization. Primary atomization refers to droplet disintegration from a continuous liquid body. Secondary atomization refers to further droplet breakup or coalescence with other droplets during the transport process. Most studies in the past have combined these two steps and treated them as one global process. For example, Rizk and Lefebvre,[1] Suyari and Lefebvre,[2] Wang and Lefebvre,[3] and others have illustrated that liquid properties of viscosity, surface tension, and density influence atomization quality. However, to better understand the atomization mechanism, it is important to examine separately the two aforementioned atomization stages. Instead of studying fluid property effects on the global atomization quality, this Technical Note focuses on the primary atomization stage of a simplex pressure-swirl spray and, specifically, investigates experimentally the effect of fluid properties on conical liquid sheet disintegration.

The phenomenon of liquid sheet disintegration has been extensively studied theoretically. In theoretical analyses, for example, Squire,[4] York et al.,[5] Hagerty and Shea,[6] Clark and Dombrowski,[7] Rangel and Sirignano,[8] Lin,[9] and Li and Tankin[10] concluded that Weber number (ratio of the inertial and interfacial surface tension forces) is an important parameter for liquid breakup and Ohnesorge number (ratio of the internal viscous force to the interfacial surface tension force) is also an important parameter if liquid viscosity is considered. The effect of Reynolds number is not explicitly discussed. In this study, the liquid sheet breakup length is not only found to be a function of Weber and Ohnesorge numbers, but is also a strong function of Reynolds number.

Experimentally, Dombrowski and Fraser[11] used a photographic technique to demonstrate that liquid sheets with high surface tension and viscosity were resistant to disruption and that the effect of liquid density on liquid sheet disintegration was small. Rizk and Lefebvre[12] also examined the mechanism of sheet disruption by using high-speed flash photography. The photographs showed that an increase in liquid viscosity resulted in a liquid sheet with fewer waves and more resistance to breakup. These experiments only demonstrated qualitatively the adverse effect of increasing fluid viscosity and surface tension on liquid sheet disintegration.

This study examines quantitatively the effect of fluid properties on discharge coefficient and breakup length of a simplex pressure-swirl nozzle. Discharge coefficient specifies the available flow rate of the nozzle and also indicates the pressure loss across the nozzle. Breakup length represents the liquid disintegration potential across the nozzle. Qualitatively, liquid sheet features, that is, the sheet surface appearance and the spray-cone shape, illustrate the spray development and relate to the atomization quality. Such studies can help one understand how an atomizer handles different fluids, so that one can maintain atomization quality.

Experimental Procedures

The experimental setup is shown schematically in Fig. 1. High-pressure nitrogen (at 690 kPa) is introduced into a stainless steel vessel to drive liquid through a 5-μm pore sintered filter, metering valve, flowmeter, and then through a hollow-cone pressure-swirl nozzle. Upstream of the atomizer, a pressure gauge is used to measure the fluid injection pressure Δp. The injection pressure was varied from 207 to 690 kPa by adjusting a metering valve. The atomizer orifice diameter d is 0.025 cm, and the nominal flow rate is 63 cm^3/min at the designed injection pressure of 860 kPa. At the nominal operating conditions, the spray forms a 60-deg cone angle.

The atomization process from a hollow-cone spray is turbulent; therefore, a single-flash stroboscope with a 3-μs pulse duration was used as a backlighting source to freeze the instantaneous disruption process. A long-distance microscope attached to a 35-mm camera was used to photograph the process. To optimize resolution and capture the region of liquid breakup, different photographic magnifications were used for different viscosity fluids. Changing the distance between the camera and objective lens varied the magnification of the microscope. The maximum magnification factor was 5 for this experimental arrangement. More than 15 photographs were taken for each experiment. Because the breakup boundary along the conical sheet varies at different circumferential locations, the breakup length was determined by choosing a specific point on a conical

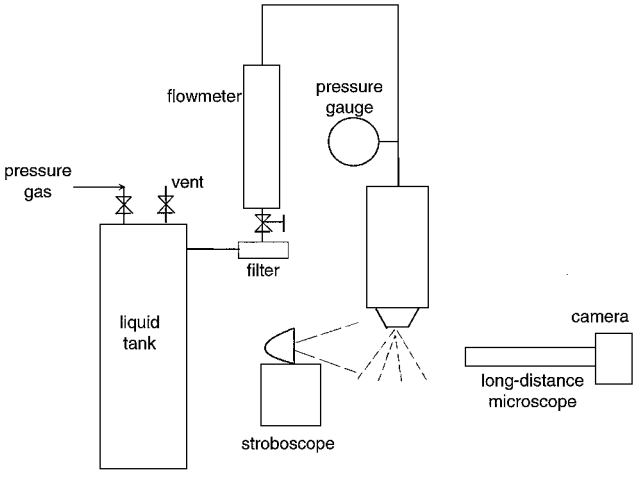

Fig. 1 Schematic of experimental setup.

Received 3 August 1999; revision received 31 March 2000; accepted for publication 3 April 2000. This material is declared a work of the U.S. Government and is not subject to copyright protection in the United States.

*Mechanical Engineer, Chemical Science and Technology Laboratory; currently Development Engineer, Technology and Commercial Development Group, John Zink Company, Koch Industries Company, 11920 E. Apache, Tulsa, OK 74121-1220.

†Leader, Thermal and Reactive Processes Group, Chemical Science and Technology Laboratory.

Table 1 Fluid physical properties

Liquid (volume fraction)	Kinematic viscosity ν, mm^2/s	Surface tension σ, kg/s^2	Density ρ, kg/m^3	Ohnesorge number Oh (10^3)
Methanol	0.9	0.023	788	10.5
Water–detergent (≈2/98)	1.0	0.048	995	9.11
Water	1.0	0.072	995	7.43
Glycerol–water (≈10/90)	1.7	0.071	1000	12.7
Kerosene	2.3	0.026	802	25.5
Glycerol–water (≈15/85)	2.3	0.070	1009	17.5
Glycerol–water (≈25/75)	4.1	0.068	1078	32.6
Glycerol–water (≈30/70)	6.0	0.062	1081	50.1

sheet and averaging the values from more than 15 photographs of the same spray. A fine-scale reticule (40 lines/mm) was used to measure the breakup length.

In this experiment, eight different fluids were used: methanol, water–detergent mixture, water, kerosene, and four different glycerol–water mixtures. The fluid properties measured at 293 K are listed in Table 1. Two pairs of fluids with the same kinematic viscosity ν but different surface tensions, that is, $\nu = 1.0$ mm^2/s for fluids 2 and 3 and $\nu = 2.3$ mm^2/s for fluids 5 and 6, were used so that the effect of surface tension was isolated from viscosity. Because the liquid density ρ from previous studies[1,3,9] was shown to have a small effect on liquid atomization, the experiments focused primarily on the influence of liquid viscosity and surface tension σ. The variation of the fluid density, therefore, was small, as shown in Table 1. The Ohnesorge number, that is, $Oh = \nu\rho/(\rho\sigma d)^{0.5}$, was also calculated and listed in Table 1, where d is the atomizer orifice diameter.

In these experiments, the liquid volume flow rate Q was measured and the liquid bulk exit velocity U_b was calculated as

$$U_b = Q/A \tag{1}$$

where A is the cross-sectional area of the atomizer orifice. From the liquid bulk exit velocity, the nozzle discharge coefficient C_D is defined as

$$C_D = U_b/(2\Delta p/\rho)^{0.5} \tag{2}$$

where Δp is the pressure drop across the atomizer. The discharge coefficient represents the ratio of the actual flow rate to the theoretical flow rate.

Results and Discussions

Sheet Features

Lefebvre[13] described the development of sprays from a low injection pressure to a high injection pressure in five stages as dribble, distorted pencil, onion, tulip, and fully developed. These five stages are given in order of increasing atomization quality. The series of photographs in Figs. 2–4 show that the parameter affecting the development of sprays is not only injection pressure, but also fluid viscosity and surface tension.

Figure 2 illustrates how the fluid 1 liquid sheet changes at three injection pressures of 207, 414, and 690 kPa. The photograph exposure time is 3 μs. Figures 2a–2c show that, with increasing pressure, the breakup length reduces and the spray cone changes from a convex surface shape (or tulip stage) to a plain surface shape (or fully developed spray). The change in the spray cone shape is attributed to the competition between the inertial force (driven by the injection pressure) and the contraction force (developed from the liquid surface tension).[13]

The effect of viscosity on the sheet features is emphasized more distinctly on the sheet surface than on the spray cone shape, as shown in Fig. 3. Four different viscosity fluids are presented with a similar value of surface tension, that is, fluids 3, 6, 7, and 8 with

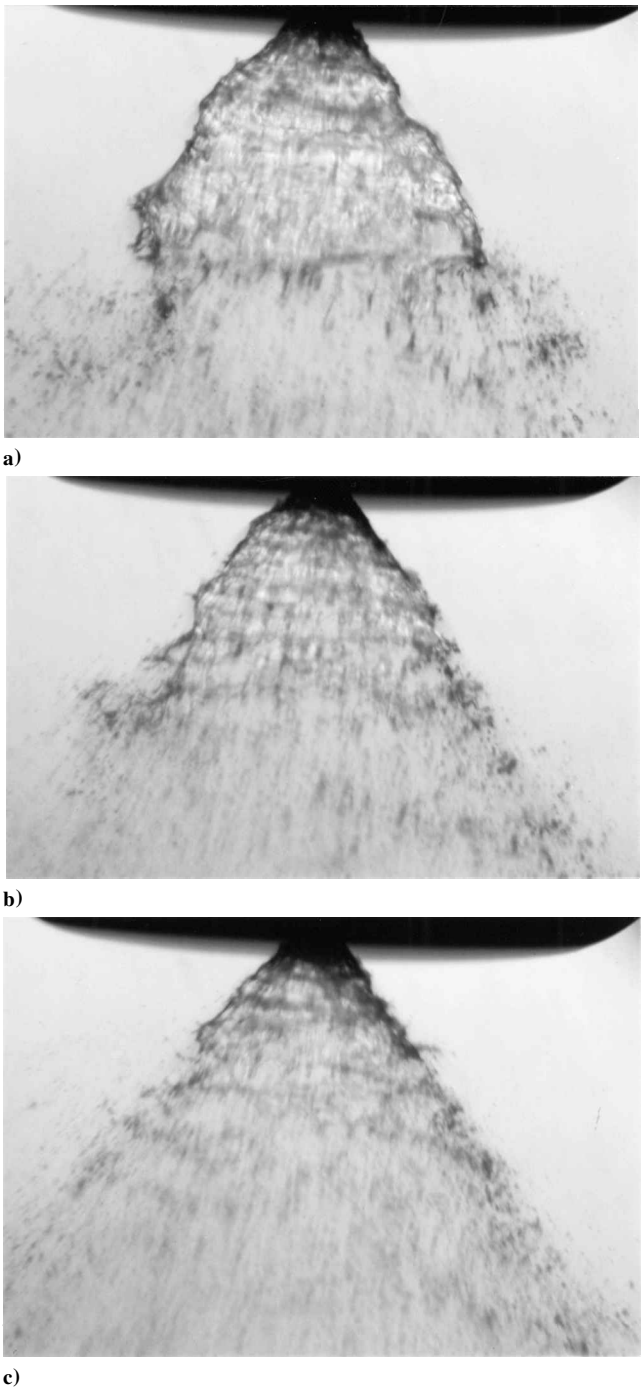

Fig. 2 Representative photographs of the spray features for fluid 1 ($\nu = 0.9$ mm^2/s, $\sigma = 0.023$ kg/s^2, and $\rho = 788$ kg/m^3) at different injection pressures Δp = a) 207 kPa, b) 414 kPa, and c) 690 kPa.

$\nu = 1.0$, 2.3, 4.1, and 6.0 mm^2/s, respectively. For lower viscosity fluids, that is, Figs. 3a and 3b, $\nu = 1.0$ and 2.3 mm^2/s, respectively, the liquid surface is turbulent with ripples at different wavelengths. In addition, a long wavelength disturbance is superimposed on the surface where its amplitude continues to grow until breakup. For a higher viscosity fluid, for instance, Fig. 3d, the waves on the surface appear more simplex and many perforated holes are observed, which become the dominant mechanism of disintegration.[14,15]

The effect of liquid surface tension on the liquid sheet features is demonstrated more clearly by looking at the spray cone shape instead of the sheet surface, as shown in Fig. 4. Figures 4a and 4b show the liquid sheet for fluids 2 and 3, respectively, at an injection pressure of 276 kPa. These two fluids have the same viscosity ($\nu =$ 1.0 mm^2/s), but different values of surface tension ($\sigma = 0.048$ kg/s^2 for fluid 2 and 0.072 kg/s^2 for fluid 3). The sheet surface shows

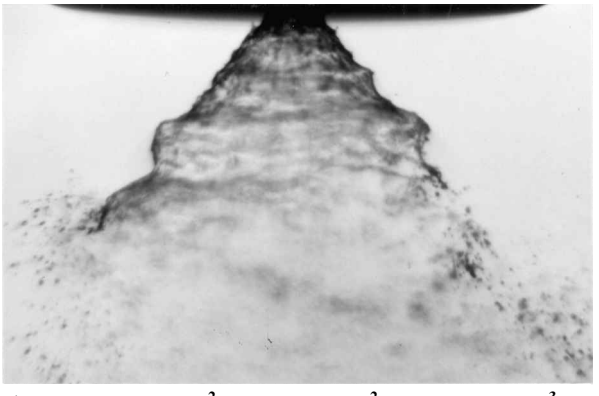

a) Fluid 3: ν = 1.0 mm^2/s, σ = 0.072 kg/s^2, and ρ = 955 kg/m^3

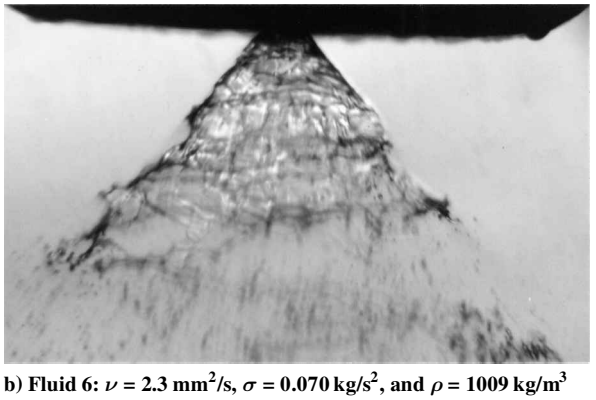

b) Fluid 6: ν = 2.3 mm^2/s, σ = 0.070 kg/s^2, and ρ = 1009 kg/m^3

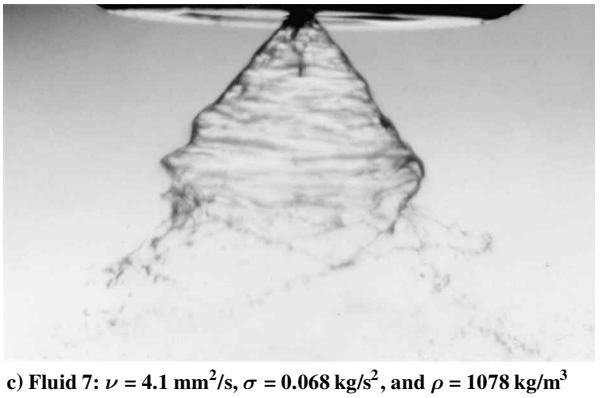

c) Fluid 7: ν = 4.1 mm^2/s, σ = 0.068 kg/s^2, and ρ = 1078 kg/m^3

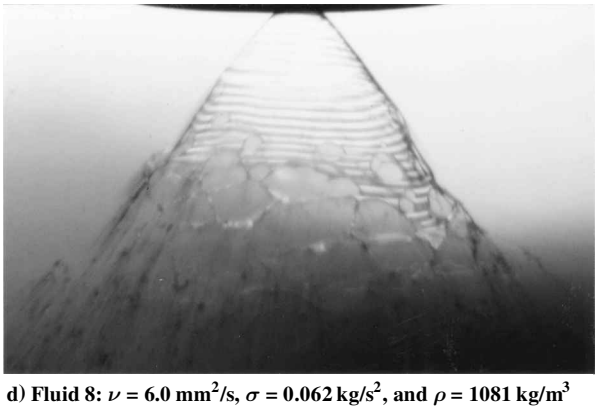

d) Fluid 8: ν = 6.0 mm^2/s, σ = 0.062 kg/s^2, and ρ = 1081 kg/m^3

Fig. 3 Representative photographs of spray features for different viscosities but similar value of surface tension at Δp = 690 kPa.

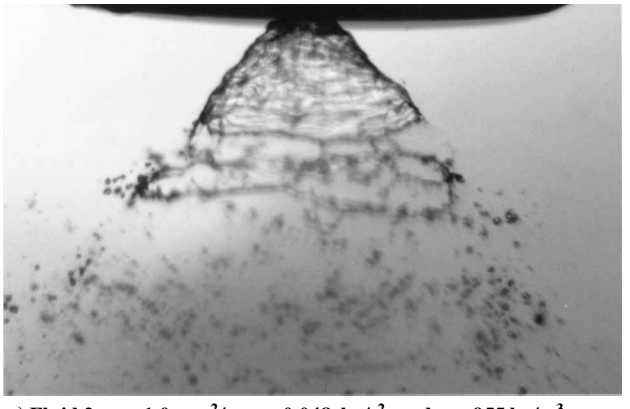

a) Fluid 2: ν = 1.0 mm^2/s, σ = 0.048 kg/s^2, and ρ = 955 kg/m^3

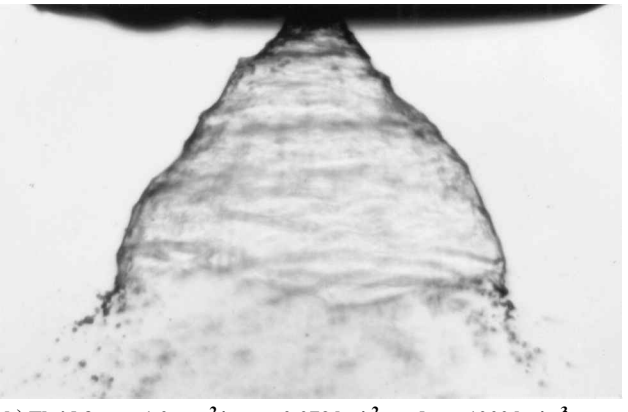

b) Fluid 3: ν = 1.0 mm^2/s, σ = 0.072 kg/s^2, and ρ = 1000 kg/m^3

Fig. 4 Representative photographs of spray features for two pairs of fluids at Δp = 276 kPa with the same viscosity but different values of surface tension.

no significant difference, but the shape of the liquid cone is different. The higher surface tension liquid generates sufficient force to contract the cone inward and produces a convex surface, as shown in Fig. 4b, whereas the lower surface tension liquid forms a plain surface cone with a shorter breakup length, as shown in Fig. 4a.

Discharge Coefficient

Many researchers have investigated the relationship between the discharge coefficient C_D of a simplex pressure-swirl nozzle and the Reynolds number. The Reynolds number was based on the orifice diameter d. For example, Radcliffe[16] studied a family of simplex pressure-swirl atomizers and demonstrated that, at low Reynolds numbers, C_D decreases with an increase of Reynolds number, and for larger Reynolds numbers, C_D is independent of the Reynolds number. In this study, a similar determination of the variation of C_D with the Reynolds number was carried out, as presented in Fig. 5. Following the methodology of other reported studies, Eqs. (1) and (2) were used to determine the value of C_D, and the Reynolds number was defined as $U_b d/\nu$. The expanded uncertainty for C_D is approximately 2% (having a 95% confidence level). Figure 5 indicates that the variation of C_D with Reynolds number is consistent with the previous studies. At low Reynolds numbers, C_D decreases with an increase of Reynolds number, and the change is reduced greatly when $Re > 2 \times 10^3$. Note that for $Re < 2 \times 10^3$ C_D is surface tension and density independent. For example, fluids 5 and 6 have different surface tensions ($\sigma = 0.026$ and 0.07 kg/s^2, respectively) and the same viscosity ($\nu = 2.3$ mm^2/s), but their values of C_D are similar for a particular value of Reynolds number. When the Reynolds number is larger than 2×10^3, however, the discharge coefficient is influenced by liquid surface tension and density. For example, fluids 2 and 3 have the same viscosity ($\nu = 1.0$ mm^2/s) but different surface tensions ($\sigma = 0.048$ and 0.072 kg/s^2, respectively). Figure 5 shows that fluid 2 with a lower surface tension has a higher value

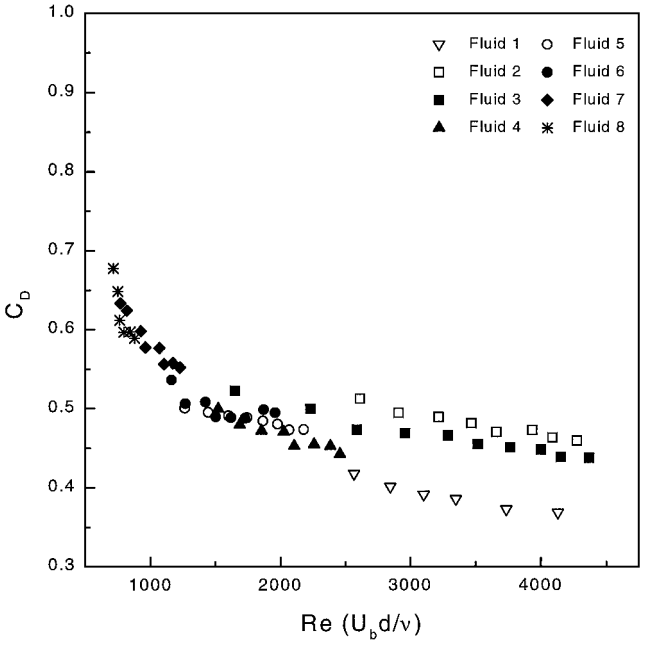

Fig. 5 Variation of the discharge coefficient of a simplex pressure-swirl atomizer with Reynolds number.

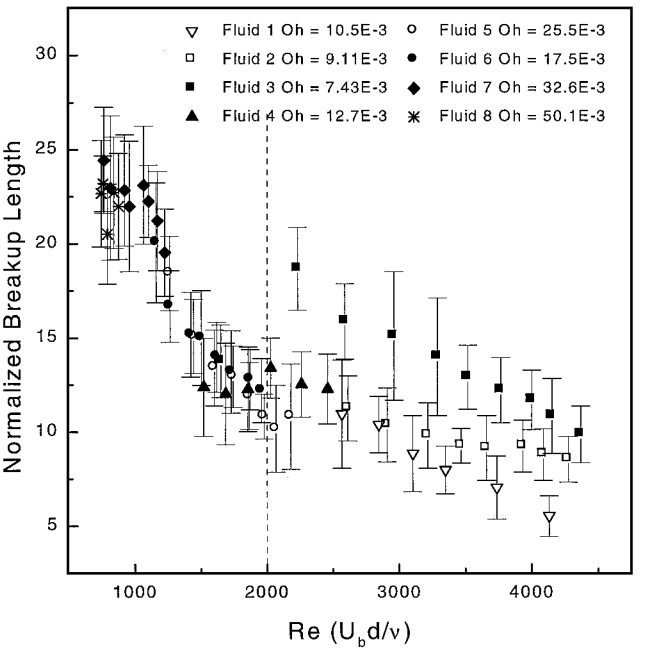

Fig. 6 Variation of the normalized liquid sheet breakup length with Reynolds number for different values of Ohnesorge number. The curve is divided into region I ($Re < 2 \times 10^3$) and region II ($Re > 2 \times 10^3$) by the vertical dashed line.

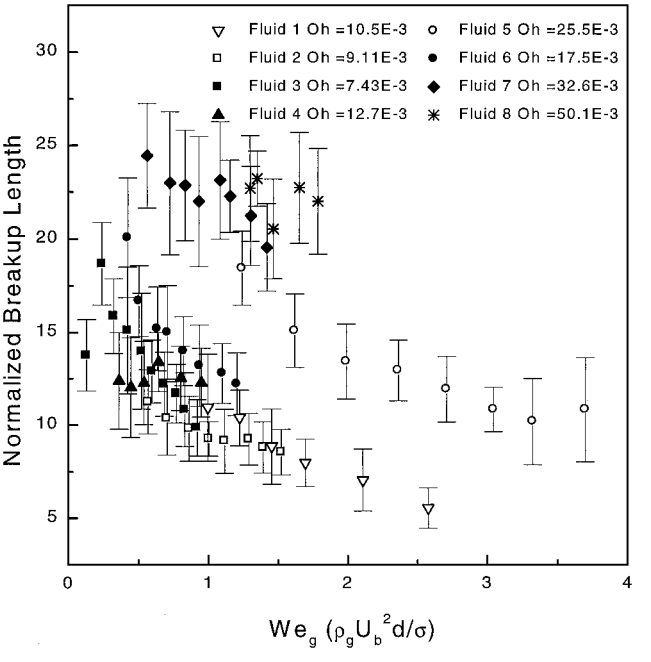

Fig. 7 Variation of the normalized liquid sheet breakup length with gas Weber number for different values of Ohnesorge number.

of C_D than fluid 3. In another case, fluid 1 ($\nu = 0.9$ mm^2/s), with a similar viscosity to fluids 2 and 3, has a lower surface tension ($\sigma = 0.023$ kg/s^2), but the discharge coefficient is lower. This trend is attributed to that fluid 1 has a lower density ($\rho = 788$ kg/m^3 for fluid 1 and 995 kg/m^3 for fluids 2 and 3). This result suggests that fluid density plays an important role, but has an opposite effect on the discharge coefficient than surface tension. Lower fluid density has a higher-theoretical exit velocity, as given by Eq. (2), and results in a lower discharge coefficient.

Breakup Length

Li and Tankin[10] investigated the effect of the liquid viscosity (by means of the Ohnesorge number) on liquid breakup length without explicitly investigating the effect of Reynolds number. To this end, the variation of breakup length with Reynolds number for different fluid properties is presented in Fig. 6. The breakup length is reported as the average value for more than 15 photographs, and the error bar represents the standard deviation. The breakup length is normalized by the atomizer orifice diameter. The Reynolds number is defined in the same fashion as it was defined for C_D, that is, $U_b d/\nu$. The results indicate the presence of two distinct regions. For $Re < 2 \times 10^3$, the breakup length decreases with an increase in Reynolds number, and it appears to be independent on Ohnesorge number. For example, fluid 5 ($\sigma = 0.026$ kg/s^2) and fluid 6 ($\sigma = 0.070$ kg/s^2) have different values of surface tension and the same viscosity, that is, $\nu = 2.3$ mm^2/s. The data are found to coincide with one another even though there is a large difference in surface tension. When $Re > 2 \times 10^3$, both Reynolds and Ohnesorge numbers influence the breakup length. At a given Reynolds number, a lower Ohnesorge number liquid is less susceptible to disruption because of a higher surface tension and leads to a longer breakup length. For example, fluid 3 ($Oh = 7.4 \times 10^{-3}$, $\sigma = 0.072$ kg/s^2) has a longer breakup length than fluid 2 ($Oh = 9.1 \times 10^{-3}$, $\sigma = 0.048$ kg/s^2) and fluid 1 ($Oh = 10.5 \times 10^{-3}$, $\sigma = 0.023$ kg/s^2); the values of viscosity are similar for these three liquids, that is, $\nu \approx 1.0$ mm^2/s.

All theoretical analyses emphasize the importance of Weber number in characterizing liquid sheet breakup. According to Li and Tankin,[10] when the gas Weber number exceeds a critical value (ρ_g/ρ), aerodynamic instability dominates the breakup process. The gas Weber number is defined as $We_g = \rho_g U_b^2 d/\sigma$, where ρ_g is the gas density. The calculated gas Weber numbers for the reported experiments vary from 0.1 to 4, which are substantially larger than the critical value, that is, $\rho_g/\rho = 0.001$ for a water sheet in atmospheric air. Therefore, the aerodynamic mode is a dominant breakup mechanism. The variation of liquid breakup length with gas Weber number is presented in Fig. 7. As Li and Tankin point out, when liquid viscosity effects are considered, Ohnesorge number, in addition to Weber number, is a parameter that characterizes sheet breakup; that is, liquid viscosity, through Ohnesorge number, acts to reduce the growth rate. Overall, the results presented in Fig. 7 are consistent with the predictions of Li and Tankin, that is, breakup length decreases with an increase in Weber number, and a liquid with a higher Ohnesorge number is more resistant to breakup. However, when the Ohnesorge number becomes small, the variation of breakup length with Ohnesorge number tends to be less distinguishable. Although the impact of the fuel swirl (formed by the atomizer swirler) has

not been discussed in the Technical Note, note that it will contribute to the conical sheet instability. Further investigation of the effect of fluid swirl velocity on breakup length is required to elucidate the relationship between breakup length and both Weber and Reynolds numbers.

Conclusions

The effect of fluid properties on the liquid sheet features, discharge coefficient, and sheet disintegration was examined experimentally with a simplex pressure-swirl atomizer. The fluid properties of viscosity and surface tension both affect the sheet features, that is, sheet surface appearance and spray cone shape. The fluid properties of viscosity, surface tension, and density affect the discharge coefficient of a pressure-swirl atomizer. For viscosity, the discharge coefficient decreases with an increase of Reynolds number, but the change is reduced significantly when the Reynolds number becomes larger than 2×10^3. When $Re > 2 \times 10^3$, both fluid density and surface tension affect the discharge coefficient.

The variation of the breakup length with Reynolds number and Ohnesorge number indicates two distinct regimes. When $Re < 2 \times 10^3$, the breakup length decreases with an increase of Reynolds number, and is independent of Ohnesorge number. Liquid viscosity is the primary factor that influences breakup in this region. When $Re > 2 \times 10^3$, both Reynolds number and Ohnesorge number affect the breakup length such that enhanced liquid inertia (via Reynolds number) reduces further the breakup length, and increased surface tension (via Ohnesorge number) enlarges breakup length. Relating breakup length to Weber and Ohnesorge numbers also supports these results with regard to the influence of liquid viscosity, surface tension, and inertia on breakup length.

References

[1]Rizk, N. K., and Lefebvre, A. H., "Internal Flow Characteristics of Simplex Swirl Atomizers," *Journal of Propulsion and Power*, Vol. 1, No. 3, 1985, pp. 193–199.

[2]Suyari, M., and Lefebvre, A. H., "Film Thickness Measurements in a Simplex Swirl Atomizer," *Journal of Propulsion and Power*, Vol. 2, No. 6, 1986, pp. 528–533.

[3]Wang, X. F., and Lefebvre, A. H., "Mean Drop Sizes from Pressure-Swirl Nozzles," *Journal of Propulsion and Power*, Vol. 3, No. 1, 1987, pp. 11–18.

[4]Squire, H. B., "Investigation of the Instability of a Moving Liquid Film," *British Journal of Applied Physics*, Vol. 4, June 1953, pp. 167–169.

[5]York, J. L., Stubbs, H. E., and Tek, M. R., "The Mechanism of Disintegration of Liquid Sheets," *Transactions of the American Society of Mechanical Engineers*, Vol. 75, Oct. 1953, pp. 1279–1286.

[6]Hagerty, W. W., and Shea, J. F., "A Study of the Stability of Plane Fluid Sheets," *Journal of Applied Mechanics*, Vol. 22, Dec. 1955, pp. 509–514.

[7]Clark, C. J., and Dombrowski, N., "Aerodynamic Instability and Disintegration of Inviscid Liquid Sheets," *Proceedings of the Royal Society of London, Series A: Mathematical and Physical Sciences*, Vol. 329, No. 1579, 1972 pp. 467–478.

[8]Rangel, R. H., and Sirignano, W. A., "The Linear and Nonlinear Shear Instability of a Fluid Sheet," *Physics of Fluids A*, Vol. 3, No. 10, 1991, pp. 2392–2400.

[9]Lin, S. P., "Stability of a Viscous Liquid Curtain," *Journal of Fluid Mechanics*, Vol. 104, March 1981, pp. 111–118.

[10]Li, X., and Tankin, R. S., "On the Temporal Instability of a Two-Dimensional Viscous Liquid Sheet," *Journal of Fluid Mechanics*, Vol. 226, May 1991, pp. 425–443.

[11]Dombrowski, N., and Fraser, R. P., "A Photographic Investigation into the Disintegration of Liquid Sheets," *Philosophical Transactions of the Royal Society of London, Series A: Mathematical and Physical Sciences*, Vol. 247, Sept. 1954, pp. 101–130.

[12]Rizk, N. K., and Lefebvre, A. H., "Influence of Liquid Film Thickness on Airblast Atomization," *Journal of Engineering for Power*, Vol. 102, No. 3, 1980, pp. 706–710.

[13]Lefebvre, A. H., *Atomization and Sprays*, Hemisphere, New York, 1989, pp. 112–117.

[14]Fraser, R. P., "Liquid Fuel Atomization," *Sixth Symposium (International) on Combustion*, Reinhold, New York, 1957, pp. 687–701.

[15]Chung, I. P., Presser, C., and Dressler, J. L., "The Effect of Piezoelectric Transducer Modulation on Liquid Sheet Disintegration," *Atomization and Sprays*, Vol. 8, No. 5, 1998, pp. 479–502.

[16]Radcliffe, A., "The Performance of a Type of Swirl Atomizer," *Proceedings of the Institution of Mechanical Engineers*, Vol. 169, No. 3, 1955, pp. 93–106.

Characteristic Gap: A New Design Criterion for Solid Rocket Motors

Daniel Chasman*
Tensor Aeronautics, San Ramon, California 94583-1948

Introduction

THIS Note reports on development of a new, more straightforward relationship between certain solid rocket motor geometric properties and the predicted pressure spike. The values of this theoretical relationship agree well with experimental data. It also demonstrates how to apply the relationship to motor design methods.

Internal ballistics formulations developed for the design of solid rocket motors (SRM) are derived from the conservative equations using either the differential or the integral form.[1–7] The latter method is more convenient because control volume selection for the internal aerodynamics is defined by the motor geometry. It is also easier to identify the origin of terms, that is, steady-state vs unsteady terms, and, thus, to keep them separated. Because the substantial derivative is decomposed into temporal and spatial terms, it is easier to monitor the mathematical rigor of the equations of motion and to apply physically meaningful simplifying assumptions to convective terms alone or to temporal terms alone. We follow the same procedure in the present study to obtain unsteady equilibrium.

Before ignition, the pressure in the chamber is ambient. As the propellant is ignited, it generates hot gas, which fills the void volume of the chamber and pressurizes it to the design pressure in the chamber, and then the gas is ejected through the nozzle. In cases where a burnt gas mass is generated in an increasingly small void volume, the chamber fills too fast, which causes a higher than designed pressure in the chamber. For propellants with pressure-dependent burn rates, such conditions create a feedback loop process that forces ever higher generated mass, which cannot be ejected at the rate of production and, thus, is stored. For a volume that is too large, on the other hand, the same given generated mass is not sufficient to pressurize the chamber to the designed pressure level. In extreme cases, the rocket motor is extinguished prematurely.

When a thrust requirement forces designers to pack more grain in a given volume to increase the mass fraction (initial to final mass of an SRM,[1–3] usually both nozzle efficiency and void volume are sacrificed. Such a design constraint applies to all sizes of SRMs, but is more dramatic in small SRMs. This constraint sets the conditions for a nonequilibrium, erosively burning motor. The main concern, then, shifts from the choice between balanced vs nonbalanced design to that of solving of the problem of how to minimize and/or predict the pressure spike in the chamber. This is an important issue not only for the motor performance but also for the case material selection, the wall thickness, and for the design safety margin. When a multinozzle design is selected, a further reduction of the void volume, otherwise available in the convergent cone of a single-nozzle design, occurs. Although this is the reason why multinozzle design improves the mass fraction, it is also what increases sensitivity to erosive burning and, thus, to pressure spike.

The present study first discusses the theoretical aspects of the concept, which follows a previous development of an unsteady-state equilibrium formulation[4] to develop a modified unsteady-state equilibrium formulation that leads to a new design criterion. Next, experimental data corroborate the theory and demonstrate its physical interpretation. The data also demonstrate how to apply the equation to motor design.

Received 26 June 1998; revision received 21 February 2000; accepted for publication 17 March 2000.

*Senior Scientist, Propulsion, 2862 Bollinger Canyon Road. Senior Member AIAA.